

Introduction

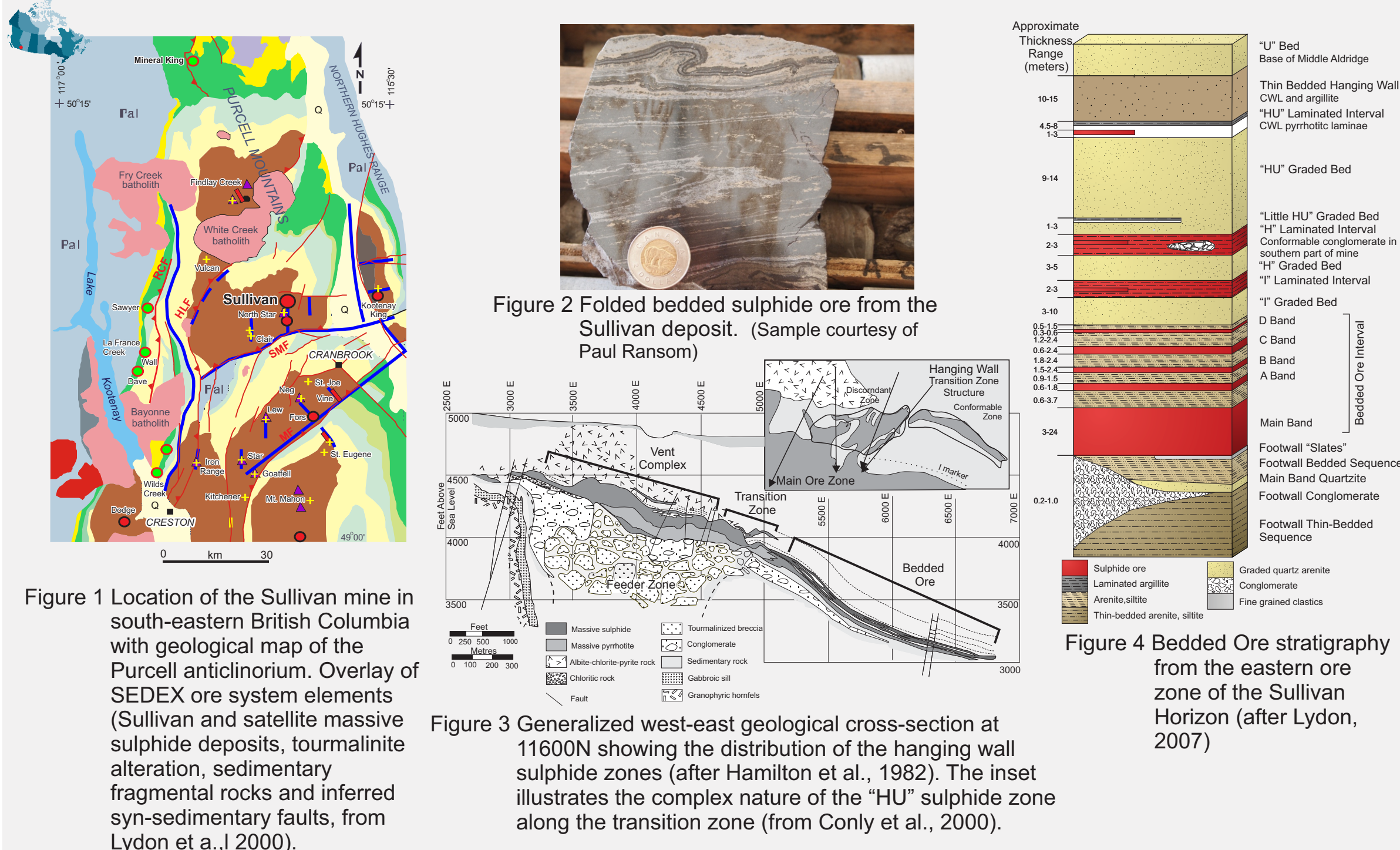
With improving technology, geologists are better at modelling and interpreting complex geological structures at depth. Previously, the mining industry interpreted geological bodies using close-spaced two dimensional sections to visualize trends in the third dimension. With the emergence of three dimensional (3D) imaging and modelling of the subsurface, the majority of modern mine records have been updated to include multi-dimensional digital models.

The Sullivan orebody, a lead and zinc SEDEX (SEDEX) deposit near Kimberley, British Columbia, was almost fully developed before the digital age. 3D modelling has been limited to small areas of active mining in the southeastern part of the deposit. This poster presents a new model which includes the entire mine site and represents metal concentrations of lead (Pb) and zinc (Zn) of the Sullivan orebody. This model is derived from horizon gridding and three dimensional kriging estimation techniques. Estimated metal zonation patterns are compared with a stratigraphic and structural 3D models of mine stratigraphy. For a more rigorous quantitative presentation see Montsion et al. (2015) and deKemp et al. (2015).

This study complements the larger regional 3D reconstruction project conducted throughout the Purcell Anticlinorium, which produced a 3D model of the Lower-Middle Aldridge Contact (LMC) and a 3D database of stratigraphic Middle-Aldridge markers (deKemp et al., 2015; Schetselaar et al., 2015; de Kemp and Schetselaar 2015).

Geological Setting

The Sullivan orebody is hosted by the Aldridge Formation of the Mesoproterozoic Belt-Purcell Basin which outcrops over an area of about 200,000 km<sup>2</sup> in Montana, Idaho and Washington of the U.S.A. and southeastern British Columbia in Canada (Lydon, 2007). The Belt-Purcell is an intracratonic rift basin and it consists of an early synrift fill sequence of deep water marine turbidites and intercalated tholeiitic sills, and a later rift sag sequence consisting of shallow marine to lagoonal and fluvial siltites, argillites, and carbonates. The syn-rift turbidite-silt sequence is named the Aldridge Formation in Canada and the Prichard Formation in the U.S.A. and is up to 12 km thick (Hoy et al., 2000). The Sullivan orebody is located on the east side of the Purcell Mountains, British Columbia and can be found in the upper part of the rift-fill succession (Figure 1).



The Sullivan orebody and its host rocks have been affected by at least two phases of tectonic and metamorphic activity (Figure 2). The first occurred during the "East Kootenay Orogeny" (1340 Ma) and the second deformation event was related to a final stage of rifting and magmatism (Lydon et al., 2000). The most significant deformation event occurred in the Cordilleran Laramide (150-110 Ma) orogeny. Local deformation effects include localized contorted folding, and tight north-south shallow plunging upright folds with slightly overturned to the east short limbs and irregular ore piercement structures as well as some low angle thrusting that can repeat mine stratigraphy.

There are two ore zone (east and west), which are separated by a structurally complex transition zone (Figure 3) (deKemp et al., 2015; Montsion et al. 2015). The western zone has been termed the 'vent complex' and is theorized to contain vents where metal enriched hydrothermal fluids emerged from the subsurface. Roughly 70% of the ore is contained within this zone. The eastern zone contains the bedded ores known as the 'Main Band', 'A Band', 'B Band', 'C Band' and 'D Band' (Figure 4) (Goodfellow and Lydon, 2007).

SEDEX Processes

SEDEX deposits form by the discharge of metalliferous hydrothermal fluids at and immediately below the sea floor of a sedimentary basin (Carne and Cathro, 1982). There has been some recent debate about how the Sullivan and other SEDEX deposits formed. Currently, there are two depositional models up for debate.

The first ore depositional model (Figure 5) postulates that once vented to the sea floor, hydrothermal fluids reacted with bacteriogenic H<sub>2</sub>S rich, anoxic, bottom water and formed a metalliferous precipitate, thereby chemically trapping the metals. The precipitate fell out of suspension and was deposited as laminated sediments and lenses along the basin floor, giving a stratiform appearance (Goodfellow and Lydon, 2007).

The second ore deposition model postulates that there was interaction between the hydrothermal fluid and sulphides in the shallow subsurface, regardless of whether the sulphides was bacteriogenic H<sub>2</sub>S, hydrothermal H<sub>2</sub>S, or pre-existing sulphide minerals. The sulphides were precipitated in pore spaces of the shallow sediments, thereby mimicking the porosity architecture of the sediments, or by replacement of pre-existing sedimentary or early diagenetic sulphides. In both ore depositional models, the resultant sulphidic rock would show sedimentary textures.

Depending on where the precipitating reaction takes place, both models of ore deposition may contribute to a single deposit (Ridley, 2013). Both mechanisms of ore deposition probably contributed to development of the rich Sullivan orebody; however the second one, the more replacement driven process may have been the dominate one.

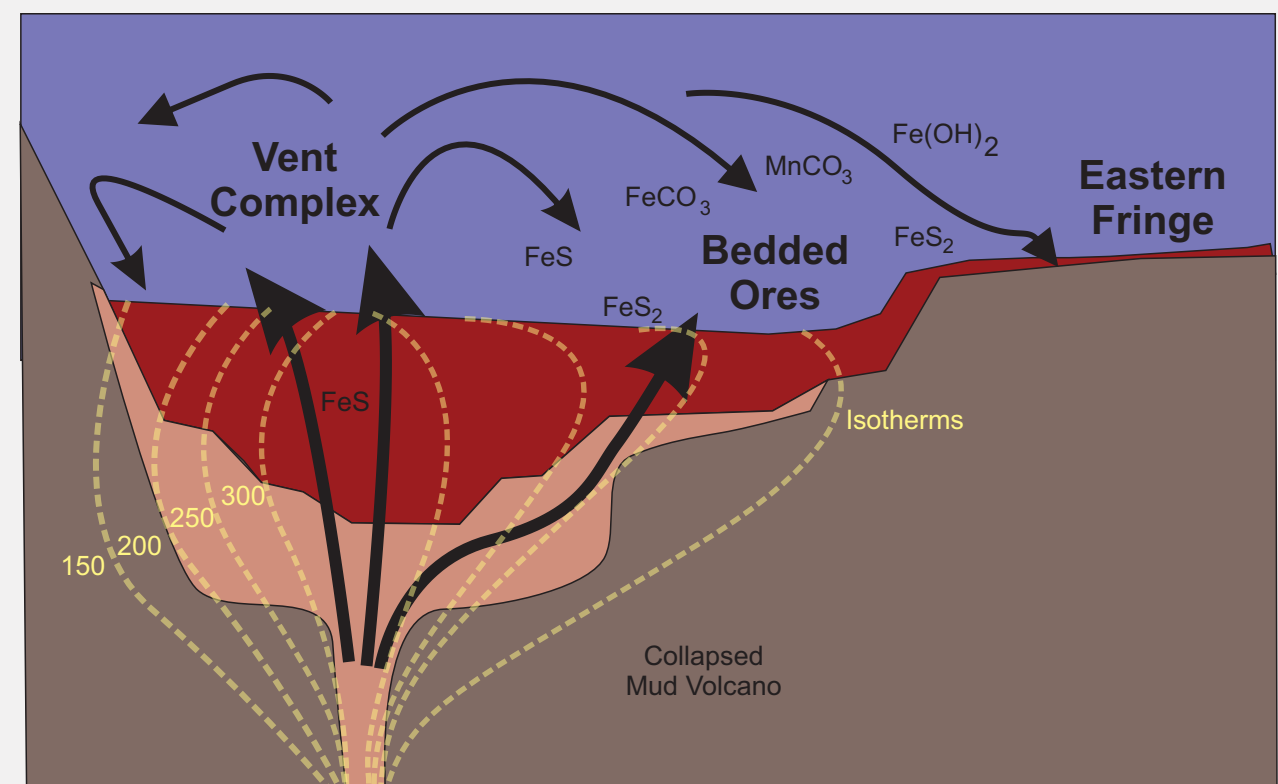
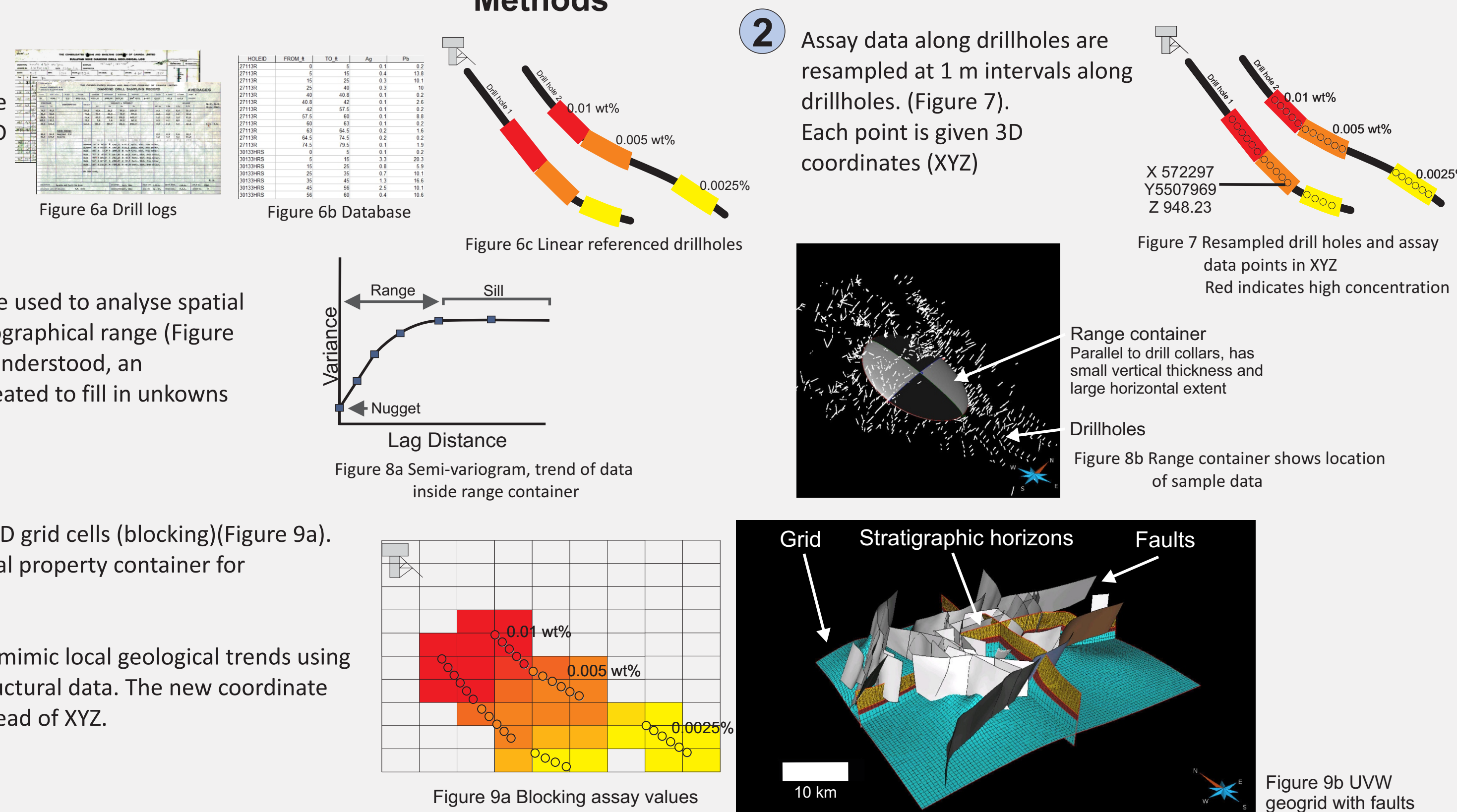


Figure 5 Model of SEDEX ore deposition of the Sullivan ore body (courtesy of Lydon)

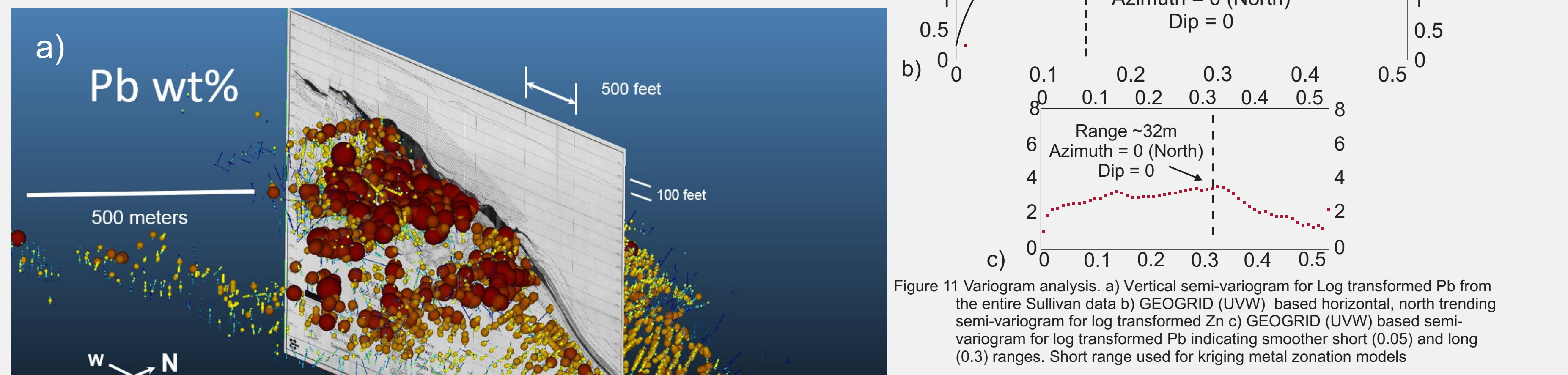
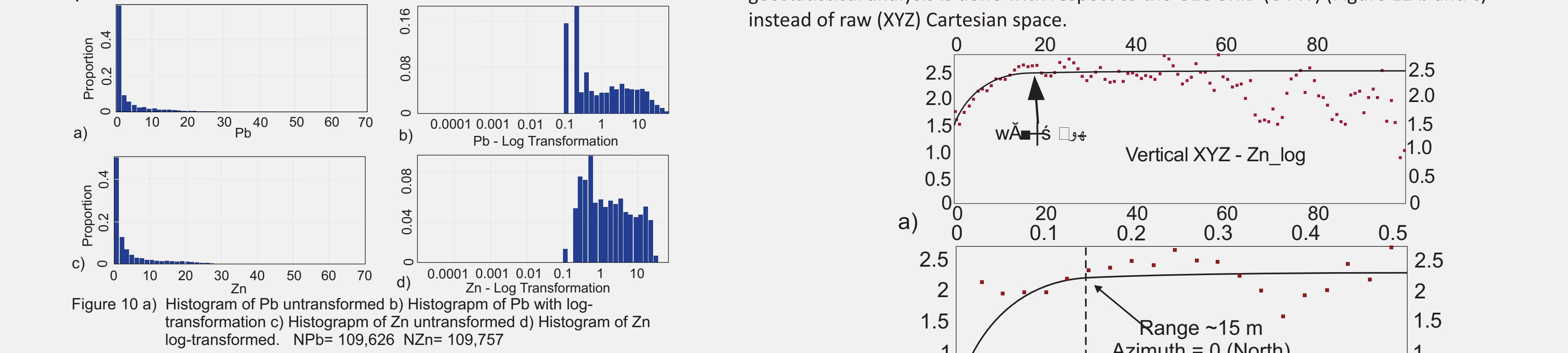
Methods

- 1 Assay data was extracted from scanned drill logs (Figure 6a), entered into a database (Figure 6b) and linear referenced to 3D drillholes (Figure 6c) from Sullivan mine survey records.
2 Assay data along drillholes are resampled at 1 m intervals along drillholes. (Figure 7). Each point is given 3D coordinates (XYZ).
3 Semi-variograms (Figure 8a) are used to analyse spatial trends in the data within a geographical range (Figure 8b). When spacial trends are understood, an interpolation model can be created to fill in unknowns between data points.
4 Metal values are assigned to 3D grid cells (blocking)(Figure 9a). The grid is then used as a metal property container for geostatistical analysis.
5 Kriging interpolation was used to visualize ore metal concentrations. Kriging algorithms use weights to linearly combine neighbouring data points to estimate unknown values. The weights are given by a computed variogram model and search parameters. To model the Sullivan's assay metal concentrations, an ordinary kriging method was selected. Ordinary kriging assumes that the interpolated property and its average will vary spatially.

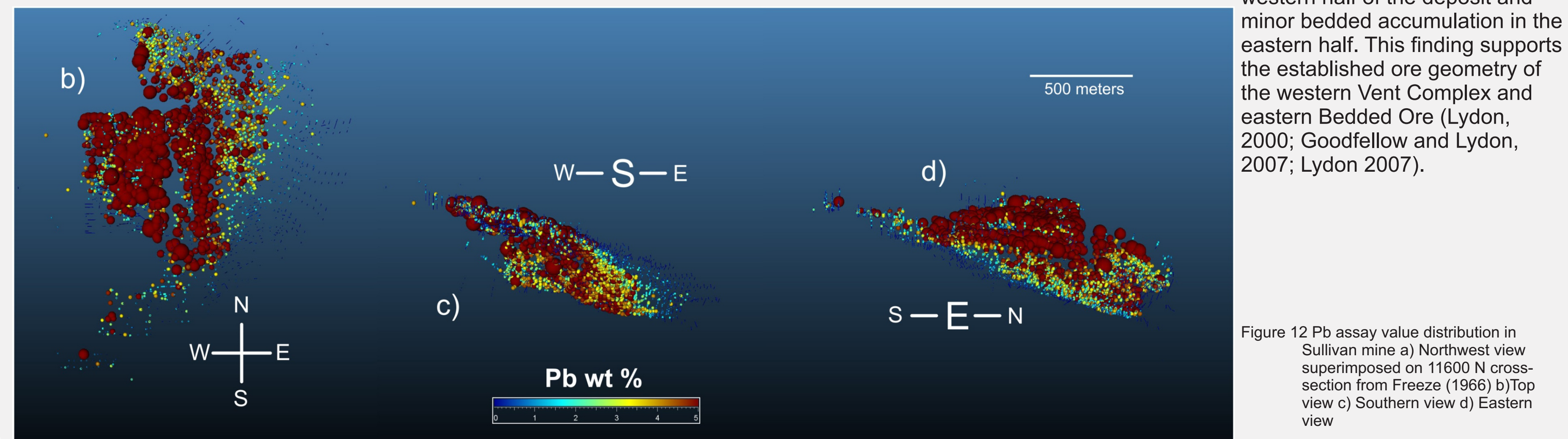


Geospatial Analysis

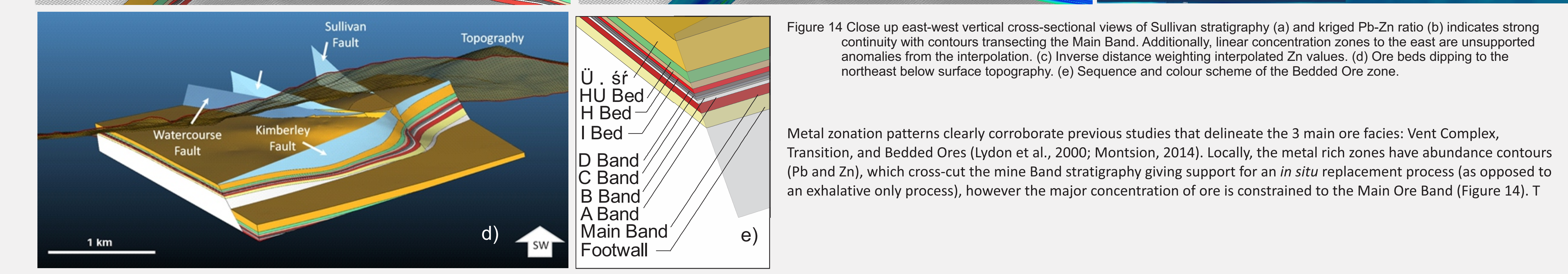
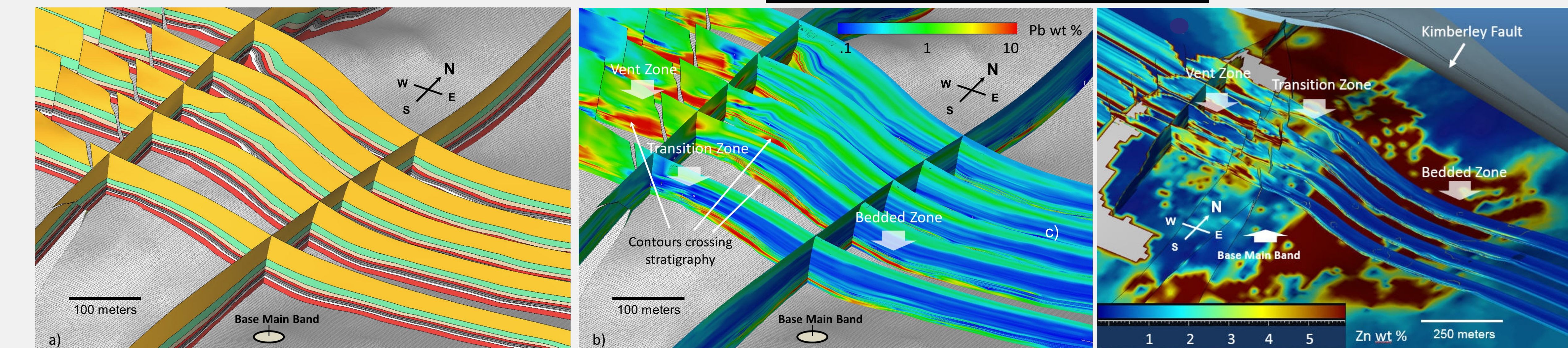
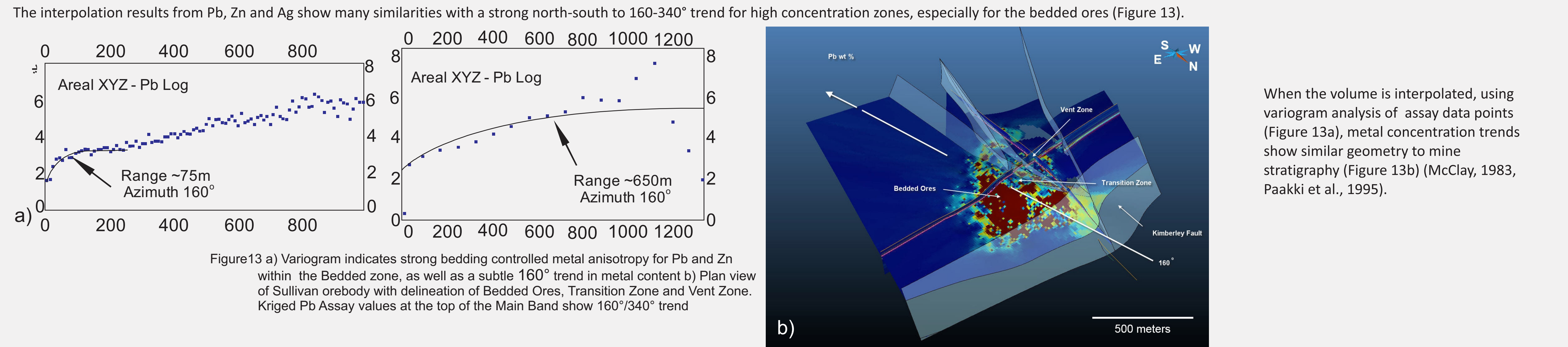
The metals Pb and Zn show a naturally skewed distribution (Figure 10 a and c). To emphasize the ore process we stretch these skewed data values with a log-transform before doing Inverse Distance Weighted (IDW) or Ordinary Kriging interpolation (Figure 10 b and d). After a metal property model is calculated, a back log transform is done to represent the natural ranges of our modelled results. Fe shows a non-skewed range of values, so we interpolate the values directly.



After linear referencing assay points to drill holes, points are symbolised to show areas of high metal concentration (Figure 12). Both metals (Pb and Zn) showed significant accumulation in the western half of the deposit and minor bedded accumulation in the eastern half. This finding supports the established ore geometry of the western Vent Complex and eastern Bedded Ore (Lydon, 2000; Goodfellow and Lydon, 2007; Lydon 2007).



Interpolation Results



When the volume is interpolated, using variogram analysis of assay data points (Figure 13a), metal concentration trends show similar geometry to mine stratigraphy (Figure 13b) (McClay, 1983; Paalkki et al., 1995). The interpolation results in Figure 13 show many similarities with a strong north-south to 160°-340° trend for high concentration zones, especially for the bedded ores. The elongate 160° trend indicated in Figure 13 by variogram analysis also matches reasonably well with several proposed syn-sedimentary graben systems from previous studies (Hagen, 1983; Höy et al., 2000; Turner et al., 2000), such as the Sullivan-Stemwinder-North Star trend, Sullivan west graben, the Clair trend, and the Star and Low trends (Moyle Block). The variograms in Figure 13 show both local and regional trends which are strongest for Pb and to a lesser extent for the other metals (Zn and Ag). There is a short ~75 metre at a 160 degree trend and a much longer regional trend in the same direction, up to at least ~650 metres.

Conclusions

- Metal zonation patterns in Figure 12 clearly corroborate previous studies that delineate the 3 main ore facies (Vent, Transition and Bedded Ore zones).
• Locally, the metal rich zones in Figure 14 have abundance contours which can transect through ore stratigraphy, supporting a replacement ore deposition model which occurred mostly in the vent and transition zone.
• The interpolation results in Figure 13 show many similarities with a strong north-south to 160°-340° trend for high concentration zones, especially for the bedded ores.
• The elongate 160° trend indicated in Figure 13 by variogram analysis also matches reasonably well with several proposed syn-sedimentary graben systems from previous studies (Hagen, 1983; Höy et al., 2000; Turner et al., 2000), such as the Sullivan-Stemwinder-North Star trend, Sullivan west graben, the Clair trend, and the Star and Low trends (Moyle Block).
• The variograms in Figure 13 show both local and regional trends which are strongest for Pb and to a lesser extent for the other metals (Zn and Ag). There is a short ~75 metre at a 160 degree trend and a much longer regional trend in the same direction, up to at least ~650 metres.
• Sullivan region, the Mine stratigraphy and geological information (lithofacies, structures, assays, and alteration) can be compared to information from regional exploration holes, since they now have a common 3D spatial framework. This could prove useful for future work in delimiting the extent of the depocentre or sub-basin hosting the Sullivan deposit, and providing leads for exploration throughout the Purcell Basin.

References

Carme, R.C., and Cathro, R.J., 1982. Sedimentary exhalative (sedex) zinc-lead-silver deposits, northern Canadian Cordillera: CIM Bulletin (1974), v. 75, no. 840, p. 66-78.
Conly, A.G., Goodfellow, W.D., Taylor, R.P., and Lydon, J.W., 2000. Geology, geochemistry and sulphur isotope geochemistry of the hanging wall sulphide zones and their related hydrothermal alteration, Sullivan Zn-Pb-Ag deposit, in Lydon, J.W., Hoy, T., Slack, J.F., and Knapp, M.E., ed., The geological environment of the Sullivan deposit, British Columbia: Geological Association of Canada, Mineral Deposits Division, Special Publication no. 1, p. 541.
de Kemp, E.A., Schetselaar, E.M., Hiller, M.J., Lydon, J.W., Ransom, P.W., Montsion, R., and Joseph, J., 2015. 3D Geological modelling of the Sullivan time horizon, Purcell Anticlinorium and Sullivan Mine, East Kootenay Region, southeastern British Columbia, in Paradis, S., ed., Targeted Geoscience Initiative 4: sediment-hosted Zn-Pb deposits: processes and implications for exploration: Geological Survey of Canada, Open File 7838, p. 236-252. doi:10.4095/296328
de Kemp, E.A. and Schetselaar, E.M., 2015. Structural and depth contours of the Lower-Middle Aldridge contact, East Kootenay Region, southeastern British Columbia: Geological Survey of Canada, 2 Map sheets geology and LMC, scale 1:100 000, Open File 7903\_1 & 7903\_2, 1 zip file.
Freeze, A.C., 1966. On the origin of the Sullivan ore body, Kimberley, British Columbia, in A Symposium on the Tectonic History and Mineral Deposits of the Western Cordillera. Canadian Institute of Mining and Metallurgy, Special Volume 8, p. 263-294.
Goodfellow, W.D., and Lydon, J.W., 2007. Sedimentary exhalative (SEDEX) deposits, in Goodfellow, W.D., ed., Mineral deposits of Canada—A synthesis of major deposit types, district metallogeny, the evolution of geological provinces, and exploration methods: Geological Association of Canada, p. 163-184.
Hagen, A.S., 1983. Sullivan-North Star graben system, unpublished report, Cominco Ltd., p. 11.
Hamilton, J.M., Bishop, D.T., Morris, H.C., and Owens, O.E., 1982. Geology of the Sullivan Orebody, Kimberley, B.C., Canada, in (ed) R.W. Hutchinson, C.D. Spence, and J.M. Franklin, Precambrian sulphide deposits: Geological Association of Canada, Special Paper 25, H.S. Robinson Memorial Volume, p. 597-665.
Hoy, T., Anderson, D., Turner, R.J.W., and Leitch, C.H.B., 2000. Tectonic, magmatic and metallogenic history of the early synrift phase of the Purcell Basin, southeastern British Columbia, in Lydon, J.W., Hoy, T., Slack, J.F., and Knapp, M.E., ed., The geological environment of the Sullivan deposit, British Columbia: Geological Association of Canada, Mineral Deposits Division, Special Publication no. 1, p. 32-60.
Lydon, J.W., 2007. Geology and metallogeny of the Belt-Purcell Basin, in Goodfellow, W.D., ed., Mineral Deposits of Canada: A Synthesis of Major Deposit Types, District Metallogeny, the Evolution of Geological Provinces, and Exploration Methods: Geological Association of Canada, Mineral Deposits Division, Special Publication No. 5, p.581-608.
Lydon, J.W., Paalkki, J.J., Anderson, H.E., and Reardon, N.C., 2000. An overview of the geology and geochemistry of the Sullivan deposit, in Lydon, J.W., Hoy, T., Slack, J.F., and Knapp, M.E., ed., The geological environment of the Sullivan deposit, British Columbia: Geological Association of Canada, Mineral Deposits Division, Special Publication no. 1, p. 505-522.
McClay, K.R., 1983. Structural evolution of the Sullivan Fe-Pb-Zn-Ag orebody, Kimberley, British Columbia, Canada. Economic Geology, v. 78, p. 1396-1424.
Montsion, R., de Kemp, E.A., Lydon, J.W., Ransom, P.W., and Joseph, J., 2015. 3D Stratigraphic, structural and metal zonation modelling of the Sullivan Mine, Kimberley, British Columbia, in Paradis, S., ed., Targeted Geoscience Initiative 4: sediment-hosted Zn-Pb deposits: processes and implications for exploration: Geological Survey of Canada, Open File 7838, p. 236-252. doi:10.4095/296328
Paalkki, J.J., Lydon, J.W., and Del Bel Belluz, N., 1995. Durchbrechung sulphides, piercement structures, and gabbro dyke displacement in the vent complex of the Sullivan Pb-Zn deposit, in Current Research 1995-A: Geological Survey of Canada, p. 81-90.
Ridley, J., Reservoir Modeling, September 2013. Ore Deposit Geology, Cambridge University Press, New York, ISBN-9781107022225
Schetselaar, E.M., de Kemp, E.A., Ransom, P.W., Buenvajiga, R., Nguyen, K., Montsion, R., and Joseph, J., 2015. Drillhole database compilation from legacy archives in support of 3D geological modelling and mineral exploration in the Purcell Anticlinorium, British Columbia, in Paradis, S., ed., Targeted Geoscience Initiative 4: sediment-hosted Zn-Pb deposits: processes and implications for exploration: Geological Survey of Canada, Open File 7838, p. 229-235. doi:10.4095/296328
Turner, R.J.W., Leitch, C.H.B., Hoy, T., Ransom, P.W., Hagen, A., and Delaney, G.D., 2000. Sullivan graben system: district-scale setting of the Sullivan deposit, in Lydon, J.W., Hoy, T., Slack, J.F., and Knapp, M.E., ed., The geological environment of the Sullivan deposit, British Columbia: Geological Association of Canada, Mineral Deposits Division, Special Publication no. 1, p. 370-407.

Acknowledgements

Many thanks to Teck (Cominco) for on site access to the Sullivan mine property and use of historical data. Thanks to Richard Laframboise (Geological Survey of Canada) who collaborated in the development of the ArcGIS Drill Core Loader software. GoCad/SKUA software support was generously provided through the GoCad Research Consortia through Paradigm® and Mira Geoscience Ltd. \* Data presented in this poster are also available from Montsion et al. 2015